Cone photoreceptors and potential UV vision in a subterranean insectivore, the European mole

Martin Glösmann
Max Planck Institute for Brain Research, Frankfurt am Main, Germany, &
Institute of Physiology, Medical University of Vienna, Vienna, Austria

Marianne Steiner
Center for Anatomy and Cell Biology, Medical University of Vienna, Vienna, Austria

Leo Peichl
Max Planck Institute for Brain Research, Frankfurt am Main, Germany

Peter K. Ahnelt
Institute of Physiology, Medical University of Vienna, Vienna, Austria

We have examined the presence, the distribution, and the opsin identity of photoreceptor types in the retina of the European mole, *Talpa europaea,* a subterranean insectivore with regressed morphology of the visual system. Cones and rods were identified using opsin antisera, and their topographies determined from flat-mounted retinas. The retina (total area 0.75 mm^2) contains about 100,000 photoreceptors, 10–12% of which are cones. Rod density is low (theoretical maximum 127,000 mm^{-2}). Cone density peaks in central retina (17,750 mm^{-2}). Similar to most mammals, two cone opsins, shortwave-sensitive (S) and middle-to-long-wave-sensitive (M), are present. Cone distribution shows a dorsoventral gradient with higher S cone numbers in ventral retina. Coexpression of S and M opsin occurs in more than 30% of the cones. Partial sequencing of the S opsin gene strongly supports UV sensitivity of the mole S cone photopigment. Amino acids that spectrally tune the S opsin are identical in *T. europaea* and in mammals with known UV cone photosensitivity. The lens transmits light down to 300 nm. Together, our data suggest that photopic vision and UV sensitivity of a cone pigment play a functional role in the European mole.

Keywords: mammalian retina, visual pigments, opsin coexpression, subterranean mammals

Citation: Glösmann, M., Steiner, M., Peichl, L., & Ahnelt, P. K. (2008). Cone photoreceptors and potential UV vision in a subterranean insectivore, the European mole. *Journal of Vision, 8*(4):23, 1–12, http://journalofvision.org/8/4/23/, doi:10.1167/8.4.23.

Introduction

The European mole, *Talpa europaea* (family Talpidae; mammalia: Eulipotyphla), is a strictly subterranean insectivore that, similar to other mammals adapted to life underground, shows anatomical regression of its visual system at several levels of organization. The eye, about 1 mm in diameter, is hidden under fur and retains a cellular lens throughout adulthood (Kriszat, 1940; Slonaker, 1902; Quilliam, 1966). The retina displays the stratified organization typical to mammals. About 2000 ganglion cells have been reported (Quilliam, 1966); the optic nerve is ~50 μm in diameter and contains ~3000 axons of which 15% are myelinated (Němec, Cveková, Burda, Benada, & Peichl, 2007). Major central targets of the eye are diminished or completely absent (Lund & Lund, 1965, 1966). Accordingly, visual capacities are considered poor, although the mole successfully performs light/dark discrimination tasks under experimental conditions (Ciba, 1995; Johannesson-Gross, 1988; Lund & Lund, 1965, 1966). Regarding the photoreceptors, two structural studies have reported a uniform population of receptors, neither rod-like nor cone-like in the classical sense (Siemen, 1976; Quilliam, 1966). Three features stand out: (i) receptors are relatively short along their radial axis, (ii) their inner and outer segments are of similar length, and (iii) the outer segments show signs of significant structural degeneration.

While the visual system of subterranean rodents has received much recent attention (for a review, see Němec et al., 2007), to date no similar studies are available for subterranean representatives of other mammalian orders. Hence, in the European mole, the presence of cones has not been explicitly confirmed yet. It is unclear whether its retina conforms to the duplex retina generally found in

doi: 10.1167/8.4.23 Received November 7, 2007; published April 23, 2008 ISSN 1534-7362

mammals, i.e., comprises rods used for low-light (scotopic) vision and cones for daylight (photopic) and color vision, or whether the mole has lost its cones in adaptation to a near-lightless visual environment. If present, do cones form two spectral types expressing shortwave (S) and middle-to-long-wave (M)-sensitive cone visual pigments as in most mammals? To address these issues, we examined the presence, the distribution, and the opsin identity of photoreceptors in the retina of *T. europaea* using opsin immunohistochemistry at the light and electron microscope level.

Materials and methods

Animals and tissue preparation

Seven adult European moles were collected in Mösbach, Germany, using tube traps under license from the Institute of Nematology and Vertebrate Research, German Federal Biological Research Centre for Agriculture and Forestry. Animals were anesthetized with diethylether, were decapitated, and heads were immersed in 4% paraformaldehyde (PFA) in 0.1 M phosphate buffer (PB, pH 7.4) from 8 hr at 4°C to 1 year at room temperature (RT). For frozen sections, eyes were cryoprotected in 30% sucrose/PB and mounted to receive vertical sections along a dorsoventral meridian. Sections (10–20 μm thick) were collected onto SuperFrost Plus slides, air dried, and stored at −30°C until use. For retinal wholemounts, five eyes were marked *in situ* at their dorsal pole. After enucleation, cornea and lens were removed, the orientation mark was transferred as a cut in the retina, and the retina was dissected free. One eye was dehydrated in graded ethanol series and embedded in London Resin White (Polysciences, Inc., Warrington, PA), and a series of sections were cut with a diamond knife on a Reichert Ultracut E ultramicrotome. Semithin sections (0.3–1 μm) were mounted on silane-coated glass slides and stained with toluidine blue. Thin sections (80–90 nm) were placed on formvar-coated gold slot grids and processed for opsin immunocytochemistry.

Light microscopic—immunocytochemical analysis

Affinity-purified rabbit antisera JH455 (raised against a human C-terminal S cone opsin epitope) and JH492 (human C-terminal M/L cone opsin epitope) were kindly supplied by J. Nathans (Johns Hopkins University School of Medicine, Baltimore; Wang et al., 1992). Monoclonal rho4D2 (against bovine rod opsin) was a gift of R. S. Molday (University of British Columbia, Vancouver; Hicks & Molday, 1986). For cone opsin double labeling, goat sc-14363 antiserum (raised against a 20-aa human N-terminal S opsin epitope; Santa Cruz Biotechnology Inc., Santa Cruz, CA) was used together with JH492. All opsin antibodies have been shown to cross-react with their mammalian homologues and were used previously to identify the respective photoreceptor types in a range of species (e.g., Peichl et al., 2005; Williams, Calderone, & Jacobs, 2005). To further confirm the specificity of the S cone markers, sc-14363 was used together with JH455. Competition controls, where sc-14363 was preincubated with antigenic peptide, yielded no labeling. Rod bipolar cells were identified on retinal sections using anti-PKCα (P4334, Sigma, St. Louis, MO) and DAPI staining. For single- or double-labeling, sections and wholemounts were blocked with 10% normal donkey serum (NDS), 0.25% Triton X-100, 0.01% NaN_3 in 0.1 M PB for 60 min at RT and incubated with primary antibodies (rho4D2, 1:500; JH455, 1:10,000; JH492 1:10,000; sc-14363, 1:200–1:1000; P4334, 1:10,000) diluted in medium (3% NDS, 0.25% Triton X-100, 0.01% NaN3 in 0.1 M PB) for 16 hr at RT. Binding sites were visualized using Alexa 488-coupled (Molecular Probes, Eugene, OR) or Cy5-coupled (Jackson ImmunoResearch Laboratories, West Grove, PA) donkey IgG (1:500; medium, 1 hr, RT). Specimens were rinsed and coverslipped in Aqua Poly/Mount (Polysciences, Warrington, PA). To apply rabbit antisera JH455 and JH492 within the same tissue, we sequentially combined the labeled avidin–biotin (LAB) technique using diaminobenzidine (DAB) as a chromogen and the indirect immunofluorescence technique. Two wholemounts were blocked with 10% normal goat serum (NGS), 3% bovine serum albumine (BSA) in 0.01 M PBS, 0.25% Triton X-100, and 0.01% sodium azide (2 hr, RT) and incubated in JH455 (1:50,000) diluted in 3% NGS, 1% BSA, 0.01 M PBS, 0.25% Triton X-100, and 0.01% sodium azide (medium) for 16 hr at 6°C. After washes in PBS/0.25% Triton X-100, retinae were incubated in biotinylated goat anti-rabbit IgG (1:300; Sigma) diluted in medium (2 hr, RT), rinsed, and processed with ExtrAvidin Peroxidase (Sigma, 1:200) in PBS/Triton X-100 (2 hr, RT). Peroxidase was visualized with DAB/H_2O_2 (0.015%/0.005%) in PBS. After rinses in PBS, the same tissue was reacted with JH492 (1:5000) in medium (16 hr, 6°C), rinsed, and incubated in Texas red-coupled goat anti-rabbit IgG (Jackson ImmunoResearch Laboratories, West Grove, PA; 1:100; 2 hr, RT). One retina was hemisected and the two pieces double labeled as follows: the dorsotemporal hemiretina was incubated in a mixture of JH455 (1:10,000) and biotinylated peanut agglutinin (PNA, 200 μg/ml; Vector Laboratories, Burlingame, CA) diluted in medium for 16 hr at 6°C. Visualization of JH455 and PNA was accomplished with Alexa 594-coupled goat anti-rabbit IgG (1:400; Molecular Probes, Eugene, OR) and ExtrAvidin FITC (1:100; Sigma), respectively, diluted in medium (2 hr, RT). The ventronasal hemiretina was similarly labeled except JH492 (1:10,000) was used as the primary antibody. Retinae were rinsed in PBS, flattened onto slides with the photoreceptor side up, and

coverslipped in Vectashield mounting medium (Vector Laboratories, Burlingame, CA).

Electron microscopic—immunocytochemical analysis

Thin sections were incubated on drops of BSA (1% in 50 mM PBS, 0.02% Tween 20) for 45 min, blotted, and single labeled for 3 hr on drops containing either the JH492 or the JH455 antiserum (1:20,000 in 1.5% NGS, 0.5% BSA, 50 mM PBS, 0.02% Tween 20). Grids were rinsed in PBS–BSA and incubated in goat anti-rabbit IgG conjugated to 5-nm gold spheres (1:20; British BioCell International, Cardiff, UK) in 1% BSA, 50 mM PBS, pH 8.0, 0.02% Tween 20) for 90 min. The grids were rinsed in buffer and distilled water, stained for 4 min with 3% uranyl acetate (aqueous solution), and viewed with an electron microscope (JEM-1200; Jeol Ltd., Tokyo, Japan).

Data collection

Cone densities and their topographic distribution were assessed from retinal wholemounts that had been sequentially immunolabeled with JH455 and JH492 to label all cones. Low power micrographs of individual retinae were acquired using a Nikon Eclipse 600 microscope coupled to a Photometrics NU-200 CCD camera and overlaid with grids of 100-μm mesh width. For positions within selected bins, cones were counted in sampling windows (97 $\times$ 97 μm) using a 100$\times$ oil immersion objective and bright-field illumination for the DAB reaction product or epifluorescence with standard filter sets for fluorochrome visualization. Unlabeled photoreceptors were identified as rods and counted using DIC optics. Shrinkage was evaluated by planimetrically determining the retinal area before and after mounting in Vectashield. Data were corrected accordingly and entered in the maps. Micrographs were taken with a Photometrics NU-200 CCD camera or made using Kodak Ektachrome 160T film and scanned. Adobe Photoshop CS (Adobe Systems, San Jose, CA) was used to adjust contrast and brightness of the images and to finally assemble figures.

Lens transmission

Lens transmission was recorded using a NanoDrop® ND-1000 UV-Vis spectrophotometer (NanoDrop Technologies, Wilmington, DE, USA). Two shortly fixed lenses of two individuals were rinsed in 0.1 M PB and clamped at 0.2-mm light path between the fiber optics of the spectrophotometer. Measurements were made at 3-nm intervals from 250 to 750 nm and normalized to 1 at 750 nm.

S opsin sequencing

Genomic DNA was extracted from ethanol-preserved muscle tissue to PCR-amplify the S opsin gene from exon 1 to exon 2 using primers 5′-CTCTGGGCCTTCCACCTC-3′ and 5′-CTGGAGCTGAAGCGGAAG-3′. Reactions were conducted in 20-μl volumes on an MJ Mini Thermal Cycler (Bio-Rad, Hercules, CA, USA) with initial denaturation at 94°C for 3 min, denaturation at 94°C for 30 s, annealing at 59.5°C for 30 s, extension at 72°C for 90 s for 35 cycles, followed by a final extension at 72°C for 5 min. A single 680 bp product was amplified, purified, and directly sequenced on both strands.

Results

General features of the mole eye and retina

In contrast to other talpid moles (e.g., *Neurotrichus gibbsii*, Lewis, 1983; *Scalopus aquaticus*, Slonaker, 1902; *T. caeca*, Niethammer, 1990), *T. europaea* has an open lid through which the minute eye (Figure 1A) can be actively protracted from the large palpebral cavity (Figure 1B). The pupil is small and the lens entirely cellular. All retinal layers are present (Figures 1B and 1C). The photoreceptor layer comprises 4–6 rows of somata. Rod and cone nuclei are indiscriminable by their size or differentially grained chromatin (Figure S2A), similar to those of non-fossorial insectivores (*Crocidura*; Peichl, Künzle, & Vogel, 2000). Photoreceptor inner segments are densely packed and of uniform size. We found no morphological criteria that enabled the unequivocal differentiation of rods and cones in the toluidine blue-stained semithin sections. Table 1 compiles the general features of the eye and the retina of *T. europaea* together with the evaluated photoreceptor properties (see below).

Rod and cone opsins

Immunostaining demonstrated that a rod opsin and two cone opsins are present in the mole retina (Figure 2). Rod opsin-specific rho4D2 labeled the majority of photoreceptors (Figure 2B). Cone opsin was detected in those approximately 10% of the receptors that were also labeled by the general cone marker PNA (data not shown). More cones were labeled by anti-human M opsin JH492 (Figure 2C) than by anti-S opsin sc-14363 or JH455 (Figure 2D). The limited availability of fresh mole retinal tissue made Western blot analysis of antibody specificity inapplicable. However, the opsin markers used in this study have been shown previously to cross-react with their mammalian homologues in a range of species and reliably identify the respective photoreceptor types (e.g., Bobu,

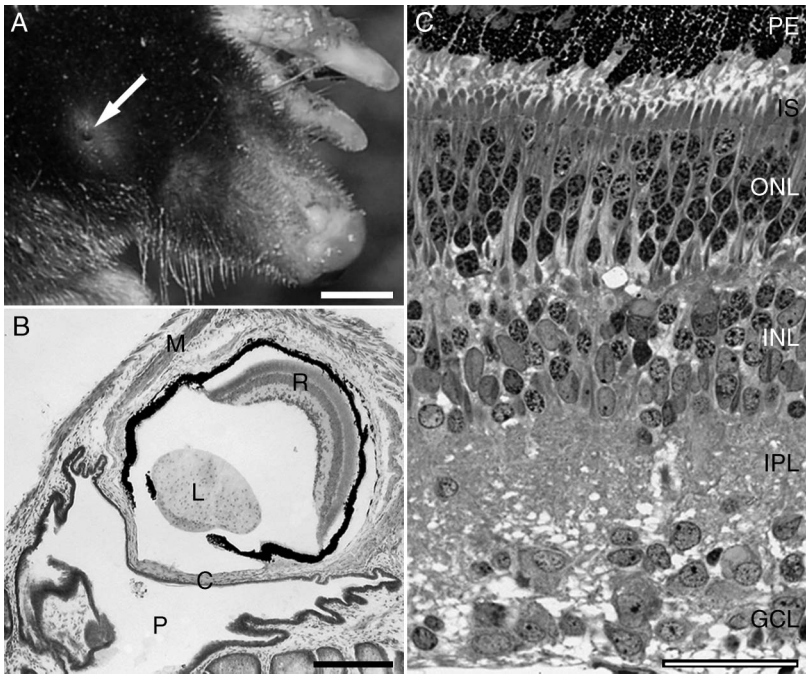

Figure 1. Eye and retina of *T. europaea*. (A) Head of an adult mole with the minute eye (arrow) protruding through the palpebral slit. (B) Mole eye and adnexa. Cresyl-violet-stained cryostat section. Peripheral retina artefactually detached from the pigment epithelium. C: cornea; L: lens; M: external eye muscle; P: palpebral cavity; R: retina. (C) Adult mole retina. Toluidine-blue-stained semithin section. PE: pigment epithelium; IS: photoreceptor inner segments; ONL: outer nuclear layer; INL: inner nuclear layer; IPL: inner plexiform layer; GCL: ganglion cell layer. Scale bars: (A) 5 mm, (B) 250 μm, (C) 30 μm.

Craft, Masson-Pevet, & Hicks, 2006; Peichl et al., 2005; Williams et al., 2005). Of note, sc-14363 and JH455, raised against a human S opsin N- and C-terminal epitope, respectively, showed complete colocalization in double labelings, albeit at different affinities, strongly supporting S opsin specificity in *T. europaea* (Figure S1).

Rod densities, cone densities, cone/rod ratios, and rod bipolar cells

Rod densities and cone/rod ratios were determined from flat-mounted whole retinae (n = 4, obtained from four individuals; Table 1) that were immunostained for cone opsin. The density of the unstained rods was assessed by DIC optics. Sampled positions included dorsal, central, and ventral retinal fields. The European mole has a rod-dominated retina with relatively high cone density (Figure 3). Rod densities ranged from 99,000 mm^{-2}, *SD* ±2000, in dorsal periphery to 109,000 mm^{-2}, *SD* ± 6000, in ventral periphery, with a density peak of 127,000 mm^{-2}, *SD* ±9000, in central retina. Total cone density increased from 10,300 mm^{-2}, *SD* ±400, in dorsal to 14,200 mm^{-2}, *SD* ±300, in ventral periphery, with a peak of 17750 mm^{-2}, *SD* ±3400, in mid-ventral retina. Cone percentages at selected positions were 9.0–15,6%, corresponding to cone/rod ratios of 1:5.4–1:10. From the sampled receptor densities, we extrapolate a total of approximately 100,000 photoreceptors per mole retina.

We identified similar frequencies of rod bipolar cells in sections of mole and rat retina (Figure S2) by labeling with anti-PKCα (Greferath, Grünert, & Wässle, 1990), demonstrating that the lower rod numbers in the mole (mole: 127,000 mm^{-2}; rat: 400,000 mm^{-2}; Hallett, 1987) are not correlated with lower rod bipolar cell densities.

Dorsoventral gradients and coexpression of S and M cone opsin

Whereas total cone density showed only a slight elevation in ventral retina (Figure 3C), S opsin expression followed a clear dorsoventral gradient (Figure 4, Figure S3). S opsin cones (i.e., cones expressing S cone opsin) increased from 2175 mm^{-2}, *SD* ±690 (n = 4), in middorsal retina to 5000 mm^{-2}, *SD* ±1000, in midventral retina, corresponding to an increase of S opsin cone proportions from approximately one to two thirds of the cones (34% to 69%; Figure S3). In peripheral retina, S opsin cone densities amounted to c. 4000 mm^{-2} and 10,000 mm^{-2} in dorsal and ventral periphery, respectively. When JH455 was used together with avidin biotin/DAB labeling, S opsin cone densities were found slightly higher (dorsal:

General	
Body weight (g)	60–80
Eye axial length/equatorial diameter (mm)	0.85/1.0
Lens diameter/thickness (mm)	0.5/0.25
Retinal diameter (mm)	1.0
Retinal area (mm^2)	0.75
Photoreceptors	
Rod density (mm^{-2})[a]	Min, 99,000, *SD* ±2000 Max, 127,000, *SD* ±9000
Cone density (mm^{-2})[a,b]	Min, 10,300, *SD* ±400 Max, 17,750, *SD* ±3400
Cone percentage of photoreceptors[c]	9.0–15.6
Dorsal total cone density (mm^{-2})[d]	11,600
Dorsal S cone percentage of cones[d]	34
Ventral total cone density (mm^{-2})[d]	14,000
Ventral S cone percentage of cones[d]	63

Table 1. Eye and photoreceptor properties of *T. europaea*. *Note*: [a]Determined in four retinae obtained from four animals at selected positions including the retinal periphery. [b]Density range across the retina. [c]Range across retina determined in four retinae at four positions each. [d]Data obtained from specimen depicted in Figure S3.

3900 mm^{-2}, ventral: 8800 mm^{-2}; mean, n = 2), presumably reflecting greater sensitivity of detection (Table 1, Figure S3). However, we identified a dorsoventral increase in S opsin cone densities regardless of the type of S opsin antiserum and the amplification protocol in use.

In contrast, M opsin cones (i.e., cones expressing M opsin) showed a markedly lower gradient. Their densities were 13,200 mm^{-2}, *SD* ±3400 (n = 4), and 16,900 mm^{-2}, *SD* ±1900 (n = 2), in dorsal and ventral retina, respectively (Table 1, Figure 4).

A significant proportion of cones colocalized S and M opsin, revealed by double-labeling with sc-14363 and JH492 (Figure 5). Three categories of cones were identified, cones expressing S opsin only, M opsin only, or, at different levels, S and M opsin (dual pigment cones). Dual pigment cones were infrequently detected in dorsal retina. Ventrally and at the retinal margins up to 80% of the S opsin cones coexpressed M opsin corresponding to a dual pigment cone percentage of c. 30% of the cones. We confirmed cone opsin coexpression in *T. europaea* using postembedding immunocytochemistry (Figure S4). Series of ultrathin sections (80–90 nm) were cut, and adjacent sections were alternately single labeled with either the JH455 or the JH492 antiserum, visualized by 5 nm gold particles. This allowed to expose the same cone outer segments to different opsin markers, avoiding cross-reaction artefacts. Adjacent sections were screened in the electron microscope and the positions of cone outer segment profiles showing immunogold signal mapped. Within transects corresponding to the ventral retina, matching profiles of cone outer segments either carried both S and M opsin signal (Figure S4A) or revealed M opsin signal only (Figure S4B). This indicates the presence of at least two cone types, one of which carries binding sites for both S and M opsin markers. In

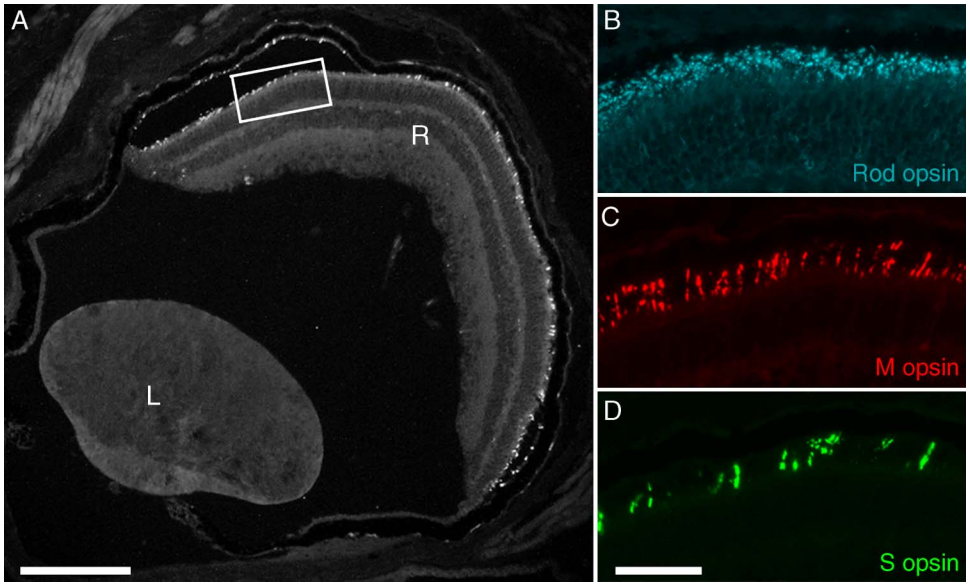

Figure 2. Rod and cone photoreceptors in the retina of *T. europaea*. (A) Vertical section of a mole eye immunostained for S opsin. Square indicates position of insets showing (B) rod opsin, (C) M opsin, and (D) S opsin immunostaining on adjacent cryostat sections. L, lens; R, retina. Scale bars: (A) 200 μm, (B–D) 50 μm.

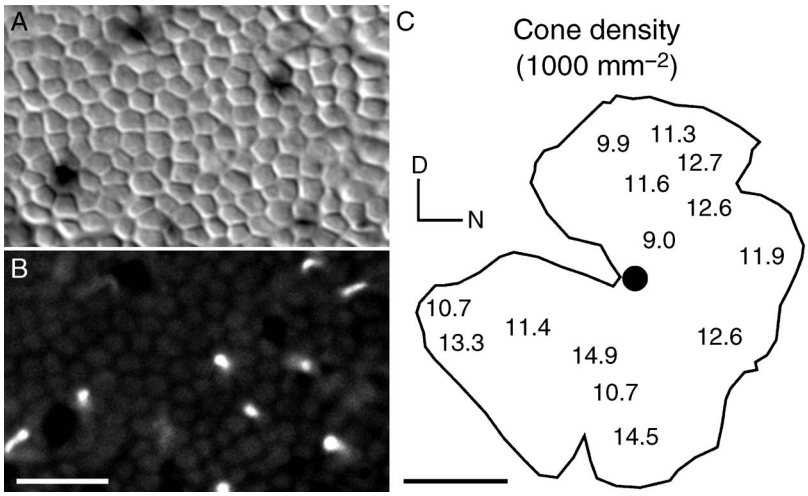

Figure 3. Cone photoreceptor topography in *T. europaea*. Micrographs showing a retinal flat-mount sequentially immunostained for S and M cone opsin to label all cones. Focus at the level of photoreceptor inner and outer segments. (A) DIC optics; S opsin cones identified by DAB. (B) Epifluorescence microscopy of same retinal field showing Texas red signal of M cones. Rods are left unlabeled by the cone opsin antibodies. (C) Cone density distribution map. D: dorsal; N: nasal. Scale bars: (B) 10 μm, (C) 250 μm.

summary, our data show that three cone types, S cones, M cones, and dual pigment cones, are present in the European mole.

Of note, opsin immunosignal was not restricted to photoreceptors (Figure S5). Rod opsin- and S opsin-immunoreactive profiles in the inner nuclear and ganglion cell layer were amacrine cell-like, a few ganglion cell layer profiles showed JH492 immunoreactivity. All S opsin-IR inner retinal neurons were colabeled by sc-14363 and JH455, suggesting misexpression of S cone opsin rather than cross-reaction artefact.

Lens transmittance

Transmittance of the whole mole lens was higher than 80% between 750 and 380 nm, decreased to 50% of its maximum at 310 nm, and dropped to 15% at 300 nm (Figure 6).

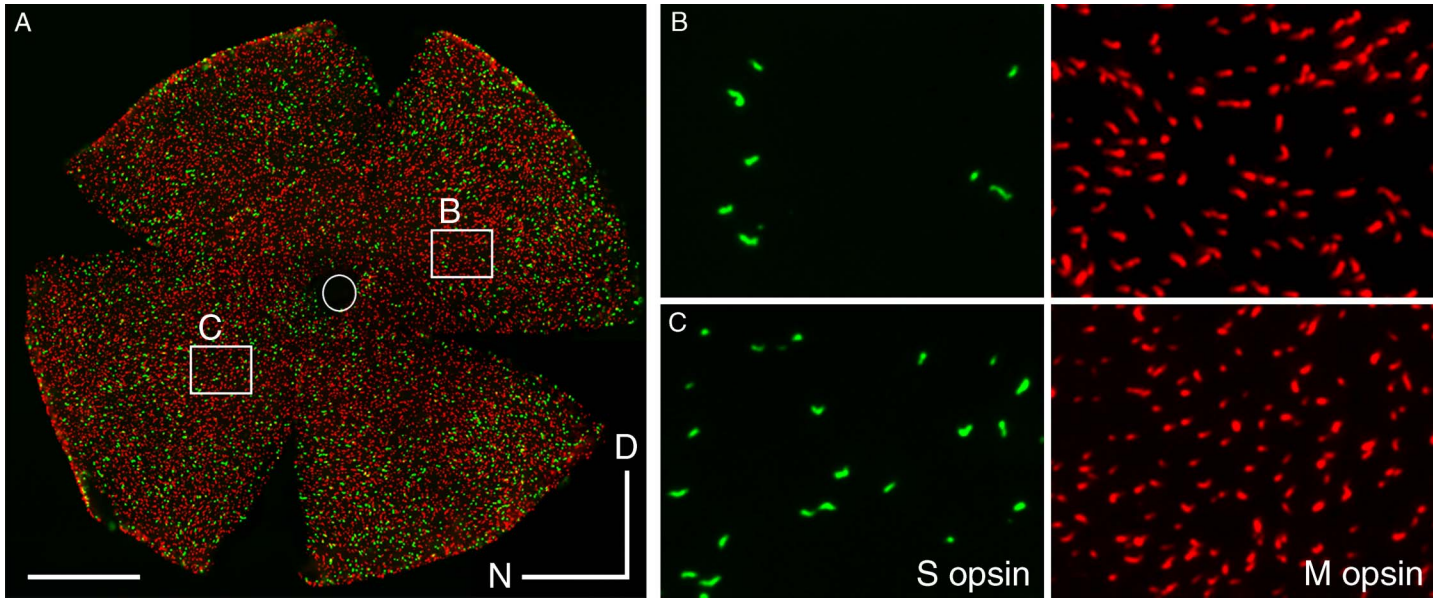

Figure 4. Topography of S and M cone opsin expression in *T. europaea*. Retinal wholemount double labeled with goat anti-S opsin sc14363 (detected with donkey anti-goat Alexa Fluor 488, green) and rabbit anti-M opsin JH492 (detected with Cy5-coupled donkey anti-rabbit IgG, red). Boxes (B) and (C) indicate the positions of enlarged areas in dorsal and ventral midretina, respectively. S cones are less numerous in dorsal retina, while M cone density follows no gradient. Cone opsin coexpression is not evident at this level of magnification. Scale bar: 200 μm.

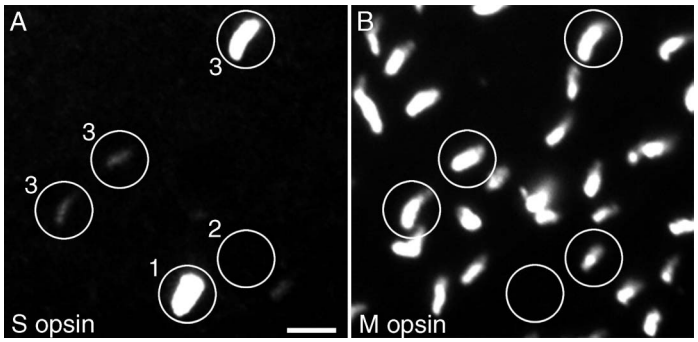

Figure 5. Coexpression of cone opsins in *T. europaea*. Fluorescent micrographs of a flat-mounted retina double labeled with markers for (A) S opsin and (B) M opsin. Indicated (circles) are cones expressing (1) only S opsin, (2) only M opsin, or (3), at different levels, S and M opsin. Scale bar: 5 μm.

S opsin molecular analysis

The S opsin gene sequence including codons critical for determining blue or ultraviolet (UV) sensitivity of the S pigment (Hunt et al., 2007) was partially obtained from genomic DNA and has been deposited in GenBank (accession number EU130563). *T. europaea* has Phe86 (Table 2), implying that a functional S pigment in the mole is UV sensitive. Phe86 is present only in UV-sensitive S pigments (mammals, e.g., mouse, rat; Yokoyama, 2000). In mammals with blue-sensitive S pigments (e.g., guinea pig, Parry, Poopalasundaram, Bowmaker, & Hunt, 2004; squirrel, Carvalho, Cowing, Wilkie, Bowmaker, & Hunt, 2006), site 86 is occupied differently.

Discussion

We have used opsin immunolabeling to demonstrate the presence of both rods and cones in the diminutive eye of *T. europaea*. Rods are dominant, and the proportions of photopic cones are 9–15%. *T. europaea* retains the full cone pigment complement, S and M, typical for dichromatic mammals. S opsin cone densities are higher in ventral retina, similar to non-fossorial insectivores (Peichl et al., 2000); however, unlike in shrews and a tenrec, a significant proportion colocalizes M opsin. We here report partial sequence data of the S opsin gene strongly implying that the mole S cone photopigment maximally absorbs in the UV.

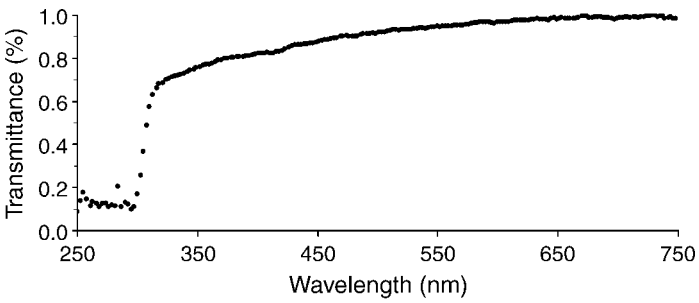

Figure 6. Transmittance of the mole lens from 250 to 750 nm, normalized to 1 at 750 nm. Shown are mean values for two lenses of two adult moles.

Species	λ_{max} (nm)	52	86	93	114	118
Homo sapiens	424	Phe	Leu	Pro	Gly	Ser
Bos taurus	438	Thr	Thr	Ile	Ala	Cys
Mus musculus	359	Thr	Phe	Thr	Ala	Ser
Rattus norvegicus	358	Thr	Phe	Thr	Ala	Ser
T. europaea	–	Thr	Phe	Thr	Ala	Ser

Table 2. Amino acids tuning the mammalian SWS1 pigment to blue or UV. *Note*: GenBank accession numbers: *H. sapiens* NM 001708; *B. taurus* NM 174567; *M. musculus* NM 007538; *R. norvegicus* NM 031015; *T. europaea* EU130563.

Rod and cone densities

Peak receptor densities determined here (156,000 mm^{-2}) closely correspond to a previous estimate of Quilliam (1966) who extrapolated a maximum of 160,000 mm^{-2} from counts in a disc-shaped central zone of high receptor density. Integration of local receptor densities suggests that approximately 100,000 photoreceptors are present in a mole eye (retinal area: 0.75 mm^2). To our knowledge, no mammal is known to possess fewer photoreceptors. In the strictly subterranean rodent *Spalax ehrenbergi*, eye size is similar to *T. europaea*, but rod and cone densities have not been assessed (Cernuda-Cernuda, DeGrip, Cooper, Nevo, & Garcia-Fernandez, 2002). Bathyergid rodents either have slightly larger eyes, and their receptor densities are unknown (*Heterocephalus glaber*, Peichl, Němec, & Burda, 2004), or significantly larger retinas with total receptor numbers increased accordingly (e.g., *Cryptomys anselli*, 3.87 mm^2 retinal area, 100,000–150,000 rods mm^{-2}, 8000–13,000 cones mm^{-2}, total receptor estimate: 500,000; data from Peichl et al., 2004).

Rod absolute frequencies in *T. europaea* (theoretical maximum 136,000 mm^{-2}) are among the lowest reported for mammals. Similar values are found in subterranean rodents. African mole rats (Bathyergidae) have 100,000–150,000 rods mm^{-2} (Peichl et al., 2004), the pocket gopher (Geomyidae) has 55,000–100,000 mm^{-2} (Williams et al., 2005). This is significantly lower than in surface-dwelling rodents. The mouse, for example, on average has 437,000 rods mm^{-2} (Jeon, Strettoi, & Masland, 1998). Are the more sensitive rods paradoxically reduced in

mammals inhabiting low-light underground environments? Comparative data do not support a convergent reduction of the rods in subterranean mammals. Rod densities (mm^{-2}) are similar, for example, in three representatives of hystricognathous rodents, the diurnal degu (*Octodon degus*, 100,000, central retina; Jacobs, Calderone, Fenwick, Krogh, & Williams, 2003), the crepuscular guinea pig (*Cavia porcellus,* 120,000–200,000, horizontal streak, 3–10% overestimate; Peichl & Gonzalez-Soriano, 1994), and the fossorial cururo (*Spalacopus cyanus*, 200,000, central retina; Peichl et al., 2005), which is certainly consistent with a role of phylogenetic constraints in shaping receptor frequencies. Rod densities vary to a larger extent in non-fossorial insectivores, with the nocturnal hedgehog (*Erinaceus europaeus*) showing up to 355,000 rods mm^{-2} (Glösmann, Harlfinger, & Ahnelt, 2001) and shrews (*Sorex*, *Crocidura*), revealing 230,000–260,000 mm^{-2} (Peichl et al., 2000), but also here, rod densities are more similar between the more closely related Soricidae and Talpidae.

A decline in rods is not paralleled by lower rod bipolar cell densities as evidenced by the similar frequencies of PKCα-positive profiles in rat and *T. europaea*. This suggests that retinal circuits supporting scotopic vision remain functional, while it remains unclear what consequences a lower convergence in the rod pathway has.

Cone numbers in the mole of 9000–21,000 mm^{-2} are similar to those in non-fossorial shrews (e.g., *Crocidura*, 9000–20,000 mm^{-2}, Peichl et al., 2000). The robust population of 10,000–12,000 cones could confer photopic capacities as discussed below.

Cone opsins

Two cone opsins (dichromacy) are ancestral to placental mammals (Hunt et al., 2007; Yokoyama, 2000) and seem also characteristic to Eulipotyphla. In contrast to the European mole, in *Spalax*, due to deletions, the S opsin gene is inexpressible (David-Gray et al., 2002). Similar to *T. europaea*, a number of subterranean rodents appear to have retained two opsins albeit with different retinal patterning. In Bathyergidae (*C. anselli*, *C. mechowi*, *H. glaber*), M opsin is barely detectable while S cones are dominant (Cernuda-Cernuda, García-Fernández, Gordijn, Bovee-Geurts, & DeGrip, 2003; Peichl et al., 2004). *S. cyanus* appears to express M and S opsin in two cone types (Peichl et al., 2005). The pocket gopher, *Thomomys bottae*, coexpresses S and M opsin in a mouse-like dorsoventral gradient (Williams et al., 2005). Thus, cone opsin patterns differ between subterranean mammals, and so far it is unclear whether species differences reflect evolutionary relationship, are adaptations in response to different visual requirements, or are neutral traits that have evolved by mechanisms other than selection.

Opsin coexpression in insectivores

While mammalian photoreceptors have long been regarded to express only one type of opsin, increasing evidence suggests that some species colocalize S and M opsins in a significant proportion of their cones. Opsin coexpression has been anatomically demonstrated in marsupials, artiodactyls, primates (including man), lagomorphs, and rodents, either permanently or transiently during early development when most cones switch expression from S to M opsin (review: Lukáts, Szabó, Röhlich, Vígh, & Szél, 2005). In mouse, two opsins within a single cone are functional (Nikonov, Kholodenko, Lem, & Pugh, 2006), and this does not obviate color vision (Jacobs, Williams, & Fenwick, 2004). While two pigments in a receptor broaden the spectral window for photon capture, the biological significance of coexpression is unknown. Here, we confirm dual pigment cones in *T. europaea*, a representative of the Soricomorpha (Eulipotyphla), and demonstrate that at least 30% of the S cones coexpress M opsin. This is in contrast to two genera of shrews and a tenrec, in which Peichl et al. (2000) found no evidence for coexpression. It is possible that coexpression affects an even larger population of cones in the mole. In fact, the different results yielded with our colocalization experiments support two different conclusions. The opsin double fluorescence labeling of frozen sections indicates the presence of genuine S cones, whereas opsin immunogold detection on ultrathin sections implies expression of M opsin in all cones with S opsin coexpressed in a subpopulation, as has been reported in tammar wallaby (Hemmi & Grünert, 1999), pig (Hendrickson & Hicks, 2002), and in several species of rodents (for a review, see Lukáts et al., 2005). It is possible that with the thin sections sampled we have missed genuine S cones, which may be sparsely distributed across the retina. Alternatively, no genuine S cones are present, and with the fluorochrome detection used for the frozen sections we have failed to detect very low levels of M opsin coexpressed in cones containing primarily the S opsin. If so, M opsin present in all retinal cones constitutes a common feature of mammalian photoreceptor organization (Applebury et al., 2000) but due to the limited sensitivity of applied methodology has escaped detection in many instances.

UV sensitivity of the mole S opsin

The binding of C-terminus-specific opsin markers to cell membrane and outer segments of photoreceptors is consistent with the expression of correctly folded, full length opsins and the formation of functional visual pigments. There are no data on the absorption properties of insectivore photopigments. Circumstantial evidence

strongly suggests that the S visual pigment in *T. europaea* is maximally sensitive in the UV. For the S opsin, our molecular analysis identifies Phe at critical amino acid (aa) site 86 implying an S cone pigment with maximum sensitivity in the UV (Hunt et al., 2007). Sequence comparisons of vertebrate S opsins and site-directed mutagenesis have firmly established a role of site 86 in tuning S pigment spectral sensitivity. Only UV-sensitive S pigments have Phe86 while non-UV S pigments are occupied differently (Cowing et al., 2002). Substitution of Phe 86 by Tyr is sufficient to shift mouse and bovine S pigment spectral sensitivity from UV to blue (Cowing et al., 2002; Fasick, Applebury, & Oprian, 2002). Conversely, substitution of site 86 by Phe turns a blue S pigment UV sensitive (e.g., guinea pig, Parry et al., 2004; tree squirrel, Carvalho et al., 2006). Other sites thought to confer UV sensitivity (Shi, Radlwimmer, & Yokoyama, 2001) are identical in *T. europaea* and species known to show UV vision (Table 2). The presence of a UV cone photopigment is consistent with the UV transmittance of the mole lens. Typically, mammalian lenses attenuate radiation below 400 nm; only mammals expressing a UV cone photopigment transmit significant amounts of UV light to the retina (Hut, Scheper, & Daan, 2000). UV sensitivity of the S pigment is considered a mammalian plesiomorphy with a shift to blue having occurred several times in different orders (Hunt et al., 2007). So far, UV vision has been confirmed only within Rodentia (for a review, see Peichl, 2005). While the biological significance of UV perception still is elusive and functional and behavioral assays will be needed to ultimately confirm UV vision in insectivores, our data together with molecular evidence obtained from marsupials (e.g., Arrese et al., 2005) and bats (Müller, Peichl, Winter, von Helversen, & Glösmann, 2007; Wang et al., 2004) strongly suggest that UV vision in mammals is more widespread than previously assumed.

Possible functional roles of cones in *Talpa*

The presence of two cone opsins suggests that photopic vision has functional significance in *T. europaea*. In fact, moles do not entirely live in total darkness. They encounter light daily when clearing debris from the tunnel system and occasionally come to surface, moving to fresh territory when burrowing conditions are difficult and food is absent (Mellanby, 1967). In contrast to *Spalax*, which is considered to be effectively blind (Cooper, Herbin, & Nevo, 1993), evidence from observations of the behavior of *T. europaea* together with evidence obtained from conditioning experiments indicates that moles respond well to photopic visual stimuli. *Talpa* withdraws in response to flashlight and successfully performs light/dark discrimination tasks provided the illumination is of sufficiently high intensity (Johannesson-Gross, 1988; Lund & Lund, 1965, 1966). The mole also appears to use intensity contrast vision for orientation when swimming (Ciba, 1995). Residual visual function in *T. europaea* is further corroborated by anatomical studies demonstrating that major retinocentral projections are vestigial but not completely absent. While projections to the superficial layers of the superior colliculus (which exerts an important function in object localization) and the nuclei of the accessory optic tract (normally used to control compensatory eye movements and to stabilize the retinal image during head movements) appear to be completely lacking, sparse projections to the lateral geniculate body (a relay nucleus for cortical perception and object identification) and pretectum (used for adjusting the size of the pupil in response to changes in light intensity) are retained (Lund & Lund, 1965, 1966). Anatomically, a homologue of the visual cortex is discernable (Rose, 1912). The retention of several central targets suggests preservation of some of the associated visual capacities. Because of the minute size of the eye, the small pupillary aperture, and the markedly cellular lens, it appears unlikely that in *T. europaea* cone function is involved in high-resolution, image-forming vision. However, functional cones might well contribute to visual capacities such as light/dark discrimination, detection of object movements, and possibly also some form of hue discrimination. It has been suggested that the main use of vision for subterranean mammals is to detect breaks in their tunnel systems, caused by disturbant predators, incidentally by large herbivores, or by corrosion, and which have to be replugged for safety (e.g., Hetling et al., 2005). Depending on the time of day, tunnel breaks would represent cone- or rod-stimulating light signals, and their detection would not require high visual acuity.

Finally, it is possible that in the mole functional cone opsin pigments subserve the non-visual task of photoperiod perception. In contrast to mole rats of the rodent families Bathyergidae (*H. glaber*) and Spalacidae (*S. ehrenbergi*), which display robust circadian rhythms entrainable by light (Rado, Wollberg, & Terkel, 1992; Riccio & Goldman, 2000), circadian behavior is lacking in the mole. In the wild, *T. europaea* displays a triphasic activity pattern with ultradian periodicity approximating 8 hr (Macdonald, Atkinson, & Blanchard, 1997). While in the mole light does not seem to play a role as Zeitgeber in regulating short-term behaviors such as locomotion, feeding, activity, and resting (Hennicke, 1996), information on photoperiod changes is required to synchronize circannual behaviors such as reproduction and migration (Kumar, 1997). Because non-photoreceptoral retinal perception providing input to the central pacemakers is not very sensitive (Berson, Dunn, & Takao, 2002), the retention of multiple photopigments may enhance the efficiency of detection under conditions where light cues are poor and of low intensity.

Acknowledgments

We are grateful to Jean Malevez and Bernd Walther for providing mole eyes and to Stefanie Heynck for technical assistance. MG was supported by a travelship grant of the Austrian Research Association.

Commercial relationships: none.
Corresponding author: Martin Glösmann.
Email: gloesmann@mpih-frankfurt.mpg.de.
Address: Max Planck Institute for Brain Research, Deutschordenstrasse 46, D-60528 Frankfurt/Main, Germany.

References

Applebury, M. L., Antoch, M. P., Baxter, L. C., Chun, L. L., Falk, J. D., Farhangfar, F., et al. (2000). The murine cone photoreceptor: A single cone type expresses both S and M opsins with retinal spatial patterning. *Neuron, 27,* 513–523. [PubMed] [Article]

Arrese, C. A., Oddy, A. Y., Runham, P. B., Hart, N. S., Shand, J., Hunt, D. M., et al. (2005). Cone topography and spectral sensitivity in two potentially trichromatic marsupials, the quokka (*Setonix brachyurus*) and quenda (*Isoodon obesulus*). *Proceedings of the Royal Society B: Biological Science, 272,* 791–796. [PubMed] [Article]

Berson, D. M., Dunn, F. A., & Takao, M. (2002). Phototransduction by retinal ganglion cells that set the circadian clock. *Science, 295,* 1070–1073. [PubMed]

Bobu, C., Craft, C. M., Masson-Pevet, M., & Hicks, D. (2006). Photoreceptor organization and rhythmic phagocytosis in the Nile rat *Arvicanthis ansorgei*: A novel diurnal rodent model for the study of cone pathophysiology. *Investigative Ophthalmology & Visual Science, 47,* 3109–3118. [PubMed] [Article]

Carvalho, L. S., Cowing, J. A., Wilkie, S. E., Bowmaker, J. K., & Hunt, D. M. (2006). Shortwave visual sensitivity in tree and flying squirrels reflects changes in lifestyle. *Current Biology, 16,* R81–R83. [PubMed]

Cernuda-Cernuda, R., DeGrip, W. J., Cooper, H. M., Nevo, E., & Garcia-Fernandez, J. M. (2002). The retina of *Spalax ehrenbergi*: Novel histologic features supportive of a modified photosensory role. *Investigative Ophthalmology & Visual Science, 43,* 2374–2383. [PubMed] [Article]

Cernuda-Cernuda, R., García-Fernández, J. M., Gordijn, M. C., Bovee-Geurts, P. H., & DeGrip, W. J. (2003). The eye of the african mole-rat *Cryptomys anselli*: To see or not to see? *European Journal of Neuroscience, 17,* 709–720. [PubMed]

Ciba, B. (1995). Die Orientierung des Maulwurfs beim Schwimmen. *Zoo-Pädagogik-Unterricht, III,* 409–416.

Cooper, H. M., Herbin, M., & Nevo, E. (1993). Ocular regression conceals adaptive progression of the visual system in a blind subterranean mammal. *Nature, 361,* 156–159. [PubMed]

Cowing, J. A., Poopalasundaram, S., Wilkie, S. E., Robinson, P. R., Bowmaker, J. K., & Hunt, D. M. (2002). The molecular mechanism for the spectral shifts between vertebrate ultraviolet- and violet-sensitive cone visual pigments. *Biochemical Journal, 367,* 129–135. [PubMed] [Article]

David-Gray, Z. K., Bellingham, J., Munoz, M., Avivi, A., Nevo, E., & Foster, R. G. (2002). Adaptive loss of ultraviolet-sensitive/violet-sensitive (UVS/VS) cone opsin in the blind mole rat (*Spalax ehrenbergi*). *European Journal of Neuroscience, 16,* 1186–1194. [PubMed]

Fasick, J. I., Applebury, M. L., & Oprian, D. D. (2002). Spectral tuning in the mammalian short-wavelength sensitive cone pigments. *Biochemistry, 41,* 6860–6865. [PubMed]

Glösmann, M., Harlfinger, P. J., & Ahnelt, P. K. (2001). S opsin-like immunoreactivity is localized to bipolar cells but not cone photoreceptors in the European hedgehog. *Investigative Ophthalmology & Visual Science, 42,* S362.

Greferath, U., Grünert, U., & Wässle, H. (1990). Rod bipolar cells in the mammalian retina show protein kinase C-like immunoreactivity. *Journal of Comparative Neurology, 301,* 433–442. [PubMed]

Hallett, P. E. (1987). The scale of the visual pathways of mouse and rat. *Biological Cybernetics, 57,* 275–286. [PubMed]

Hemmi, J. M., & Grünert, U. (1999). Distribution of photoreceptor types in the retina of a marsupial, the tammar wallaby (*Macropus eugenii*). *Visual Neuroscience, 16,* 291–302. [PubMed]

Hendrickson, A., & Hicks, D. (2002). Distribution and density of medium- and short-wavelength selective cones in the domestic pig retina. *Experimental Eye Research, 74,* 435–444. [PubMed]

Hennicke, J. (1996). *Untersuchungen zur ultradianen Aktivitätsrhythmik des europäischen Maulwurfs, Talpa europaea L.* Diploma Thesis, LMU München.

Hetling, J. R., Baig-Silva, M. S., Comer, C. M., Pardue, M. T., Samaan, D. Y., Qtaishat, N. M., et al. (2005). Features of visual function in the naked mole-rat *Heterocephalus glaber*. *Journal of Comparative Physiology A: Neuroethology, Sensory, Neural, and Behavioral Physiology, 191,* 317–330. [PubMed]

Hicks, D., & Molday, R. S. (1986). Differential immunogold-dextran labeling of bovine and frog rod and cone cells using monoclonal antibodies against bovine

rhodopsin. *Experimental Eye Research, 42,* 55–71. [PubMed]

Hunt, D. M., Carvalho, L. S., Cowing, J. A., Parry, J. W., Wilkie, S. E., Davies, W. L., et al. (2007). Spectral tuning of shortwave-sensitive visual pigments in vertebrates. *Photochemistry and Photobiology, 83,* 303–310. [PubMed]

Hut, R. A., Scheper, A., & Daan, S. (2000). Can the circadian system of a diurnal and a nocturnal rodent entrain to ultraviolet light? *Journal of Comparative Physiology A: Sensory, Neural, and Behavioral Physiology, 186,* 707–715. [PubMed]

Jacobs, G. H., Calderone, J. B., Fenwick, J. A., Krogh, K., & Williams, G. A. (2003). Visual adaptations in a diurnal rodent, *Octodon degus*. *Journal of Comparative Physiology A: Neuroethology, Sensory, Neural, and Behavioral Physiology, 189,* 347–361. [PubMed]

Jacobs, G. H., Williams, G. A., & Fenwick, J. A. (2004). Influence of cone pigment coexpression on spectral sensitivity and color vision in the mouse. *Vision Research, 44,* 1615–1622. [PubMed]

Jeon, C. J., Strettoi, E., & Masland, R. H. (1998). The major cell populations of the mouse retina. *Journal of Neuroscience, 18,* 8936–8946. [PubMed] [Article]

Johannesson-Gross, K. (1988). Brightness discrimination of the mole (*Talpa europaea* L.) in learning experiments applying a modified tube-maze method. *Zeitschrift für Säugetierkunde, 53,* 193–201.

Kriszat, G. (1940). Untersuchungen zur Sinnesphysiologie, Biologie und Umwelt des Maulwurfs (*Talpa europaea* L.). *Zeitschrift für Morphologie und Ökologie der Tiere, 36,* 446–511.

Kumar, V. (1997). Photoperiodism in higher vertebrates: An adaptive strategy in temporal environment. *Indian Journal of Experimental Biology, 35,* 427–437. [PubMed]

Lewis, T. H. (1983). The anatomy and histology of the rudimentary eye of Neurotrichus. *Northwest Science, 57,* 8–15.

Lukáts, A., Szabó, A., Röhlich, P., Vígh, B., & Szél, A. (2005). Photopigment coexpression in mammals: Comparative and developmental aspects. *Histology and Histopathology, 20,* 551–574. [PubMed]

Lund, R. D., & Lund, J. S. (1965). The visual system of the mole, Talpa europaea. *Experimental Neurology, 13,* 302–316. [PubMed]

Lund, R. D., & Lund, J. S. (1966). The central visual pathways and their functional significance in the mole (*Talpa europaea*). *Journal of Zoology, 149,* 95–101.

Macdonald, D. W., Atkinson, R. P. D., & Blanchard, G. (1997). Spatial and temporal patterns in the activity of European moles. *Oecologia, 109,* 88–97.

Mellanby, K. (1967). Food and activity in the mole *Talpa europaea*. *Nature, 215,* 1128–1130. [PubMed]

Müller, B., Peichl, L., Winter, Y., von Helversen, O., & Glösmann, M. (2007). Cone photoreceptors and ultraviolet vision in the flower bat Glossophaga soricina (Microchiroptera, Phyllostomidae). *Investigative Ophthalmology & Visual Science, 43,* ARVO E-Abstract 5951.

Němec, P., Cveková, P., Burda, H., Benada, O., & Peichl, L. (2007). Visual systems and the role of vision in subterranean rodents: Diversity of retinal properties and visual system designs. In S. Begall, H. Burda, & C. E. Schleich (Eds.), *Subterranean rodents: News from underground* (pp. 129–160). Heidelberg: Springer.

Niethammer, J. (1990). *Talpa*. In J. Niethammer & F. Krapp (Eds.), *Handbuch der Säugetiere Europas, Vol. 3 Insektenfresser, Herrentiere* (pp. 93–161). Wiesbaden: AULA Verlag.

Nikonov, S. S., Kholodenko, R., Lem, J., & Pugh, E. N., Jr. (2006). Physiological features of the S- and M-cone photoreceptors of wild-type mice from single-cell recordings. *Journal of General Physiology, 127,* 359–374. [PubMed] [Article]

Parry, J. W., Poopalasundaram, S., Bowmaker, J. K., & Hunt, D. M. (2004). A novel amino acid substitution is responsible for spectral tuning in a rodent violet-sensitive visual pigment. *Biochemistry, 43,* 8014–8020. [PubMed]

Peichl, L. (2005). Diversity of mammalian photoreceptor properties: Adaptations to habitat and lifestyle? *Anatomical Record. A, Discoveries in Molecular, Cellular, and Evolutionary Biology, 287,* 1001–1012. [PubMed]

Peichl, L., Chavez A. E., Ocampo, A., Mena, W., Bozinovic, F., & Palacios A. G. (2005). Eye and vision in the subterranean rodent cururo (*Spalacopus cyanus,* Octodontidae). *Journal of Comparative Neurology, 486,* 197–208. [PubMed]

Peichl, L., & Gonzáles-Soriano, J. (1994). Unexpected presence of neurofilaments in axon-bearing horizontal cells of the mammalian retina. *Journal of Neuroscience, 13,* 4091–4100. [PubMed] [Article]

Peichl, L., Künzle, H., & Vogel, P. (2000). Photoreceptor types and distributions in the retinae of insectivores. *Visual Neuroscience, 17,* 937–948. [PubMed]

Peichl, L., Němec, P., & Burda, H. (2004). Unusual cone and rod properties in subterranean African mole-rats (Rodentia, Bathyergidae). *European Journal of Neuroscience, 19,* 1545–1558. [PubMed]

Quilliam, T. A. (1966). The problem of vision in the ecology of *Talpa europaea*. *Experimental Eye Research, 5,* 63–78. [PubMed]

Rado, R., Wollberg, Z., & Terkel, J. (1992). Sensitivity to light of the blind mole-rat: Behavioral and neuroanatomical study. *Israel Journal of Zoology, 38,* 323–331.

Riccio, A. P., & Goldman, B. D. (2000). Circadian rhythms of locomotor activity in naked mole-rats (*Heterocephalus glaber*). *Physiology & Behavior, 71,* 1–13. [PubMed]

Rose, M. (1912). Histologische Lokalisation der Großhirnrinde bei kleinen Säugetieren. *Journal für Psychologie und Neurologie, 19,* 391–479.

Shi, Y., Radlwimmer, F. B., & Yokoyama, S. (2001). Molecular genetics and the evolution of ultraviolet vision in vertebrates. *Proceedings of the National Academy of Sciences of the United States of America, 98,* 11731–11736. [PubMed] [Article]

Siemen, D. (1976). Elektronenmikroskopische Untersuchungen zur Reduktion des Auges bei unterirdisch lebenden oder nachtaktiven Säugetieren (*Talpa europaea* LINNÉ, 1758, *Erinaceus europaeus* LINNÉ, 1758, *Echinops telfairi* MARTIN, 1838). Universität Kiel: Diploma Thesis.

Slonaker, J. R. (1902). The eye of the common mole, *Scalops aquaticus machrinus*. *Journal of Comparative Neurology, 12,* 335–366.

Wang, D., Oakley, T., Mower, J., Shimmin, L. C., Yim, S., Honeycutt, R. L., et al. (2004). Molecular evolution of bat color vision genes. *Molecular Biology and Evolution, 21,* 295–302. [PubMed] [Article]

Wang, Y., Macke, J. P., Merbs, S. L., Zack, D. J., Klaunberg, B., Benett, J., et al. (1992). A locus control region adjacent to the human red and green visual pigment genes. *Neuron, 9,* 429–440. [PubMed]

Williams, G. A., Calderone, J. B., & Jacobs, G. H. (2005). Photoreceptors and photopigments in a subterranean rodent, the pocket gopher (*Thomomys bottae*). *Journal of Comparative Physiology A: Neuroethology, Sensory, Neural, and Behavioral Physiology, 191,* 125–134. [PubMed]

Yokoyama, S. (2000). Molecular evolution of vertebrate visual pigments. *Progress in Retinal and Eye Research, 19,* 385–419. [PubMed]